

# Abundances and Distributions of the Dominant *nifH* Phylotypes in the Northern Atlantic Ocean<sup>∇†</sup>

Rebecca J. Langlois, Diana Hümmer, and Julie LaRoche\*

Leibniz Institute for Marine Sciences, Duesternbrooker Weg 20, 24105 Kiel, Germany

Received 26 July 2007/Accepted 22 January 2008

Understanding the factors that influence the distribution and abundance of marine diazotrophs is important in order to assess their role in the oceanic nitrogen cycle. Environmental DNA samples from four cruises to the North Atlantic Ocean, covering a sampling area of 0°N to 42°N and 67°W to 13°W, were analyzed for the presence and amount of seven *nifH* phylotypes using real-time quantitative PCR and TaqMan probes. The cyanobacterial phylotypes dominated in abundance (94% of all *nifH* copies detected) and were the most widely distributed. The filamentous cyanobacterial type, which included both *Trichodesmium* and *Katagnymene*, was the most abundant (51%), followed by group A, an uncultured unicellular cyanobacterium (33%), and gamma A, an uncultured gammaproteobacterium (6%). Group B, unicellular cyanobacterium *Crocospaera*, and group C *Cyanothece*-like phylotypes were not often detected (6.9% and 2.3%, respectively), but where present, could reach high concentrations. Gamma P, another uncultured gammaproteobacterium, was seldom detected (0.5%). Water temperature appeared to influence the distribution of many *nifH* phylotypes. Very high (up to  $1 \times 10^6$  copies liter<sup>-1</sup>) *nifH* concentrations of group A were detected in the eastern basin (25 to 17°N, 27 to 30°W), where the temperature ranged from 20 to 23°C. The highest concentrations of filamentous phylotypes were measured between 25 and 30°C. The uncultured cluster III phylotype was uncommon (0.4%) and was associated with mean water temperatures of 18°C. Diazotroph abundance was highest in regions where modeled average dust deposition was between 1 and 2 g/m<sup>2</sup>/year.

Input and removal of fixed nitrogen in the ocean are largely controlled by the microbial processes of dinitrogen fixation and anaerobic ammonia oxidation and denitrification, respectively (23). Global rate estimates of both input and removal processes do not balance and suggest a net loss of fixed nitrogen from oceanic systems (11, 16). One reason for the imbalance of the marine nitrogen budget may be due to the paucity of data for marine diazotrophs. Until recently, the filamentous, non-heterocystous cyanobacterium *Trichodesmium* and the diatom endosymbiont *Richelia* were considered the major diazotrophs in the world's oceans (28, 49). However, field measurements and geochemical estimates indicate that these two species together do not fix enough nitrogen to balance the global marine nitrogen budget (3, 20). Methodological advances have led to the discovery of many new marine diazotrophs, and it is now possible to detect diverse diazotrophs by PCR analysis of the *nifH* gene, which encodes the highly conserved iron-protein subunit of the nitrogenase enzyme (22, 25, 26, 45, 47).

Although our knowledge of *nifH* sequence diversity from the marine environment has been rapidly expanding (46, 48), the temporal and spatial distributions of the various *nifH* phylotypes remain poorly characterized (22) and estimates of *nifH* abundances are rare. Real-time quantitative PCR (qPCR) was successfully used to determine the abundances of two *nifH* sequences at three stations in the Chesapeake Bay (39) and

five *nifH* phylotypes at Station ALOHA in the Pacific Ocean (9, 10, 38). Diazotrophs in the Sargasso Sea and Amazon River plume have also been investigated using the qPCR technique (13, 17). Although the geographical coverage was limited in each of these studies, patterns in the vertical, temporal, and seasonal distributions of *nifH* phylotypes could be identified.

The goal of this study was to determine the abundances and distributions of seven different *nifH* phylotypes over a wide geographical area of the North Atlantic ranging from the equator to 42°N. Gene copy numbers of four cyanobacterial (one filamentous and three unicellular) and two gammaproteobacterial phylotypes and one cluster III *nifH* phylotype were quantified using qPCR and TaqMan MGB probes, providing estimates of the relative distributions and abundances of these unique diazotroph groups. Our results and those of others (14, 17, 24) suggest that diazotrophy may not be as tightly constrained by geographic location as previously thought.

## MATERIALS AND METHODS

**Sample collection, nucleic acid extraction, and *nifH* amplification.** Samples for this study were collected and analyzed from four cruises in the northern Atlantic Ocean. Samples were collected in the spring during the F/S *Meteor* 60/5 Transient Tracers Revisited cruise (March and April 2004) to the North Atlantic Ocean and the F/S *Poseidon* 284 cruise (March 2002) to the eastern subtropical Atlantic Ocean. Samples along a transect at 10°N with a second transect to the equator and back were collected during the F/S *Meteor* 55 cruise (October to November 2002). Samples were collected from the F/S *Sonne* 152 cruise (November to December 2000) in the western tropical Atlantic basin. All samples were collected using a CTD rosette except for samples from the *Sonne* 152 cruise and three samples from *Meteor* 55, which were collected using an overboard pump from a depth of 8 m and a trace-metal clean diaphragm pump, respectively. *Poseidon* 284 samples were collected from depths ranging from 10 to 30 m. Samples from both *Meteor* cruises were collected at the surface (5 m) and from one to two depths ranging from 20 to 120 m. After collection, water was filtered onto 0.22- $\mu$ m Durapore (Millipore) filters under low (2 mbar) vacuum pressure

\* Corresponding author. Mailing address: Leibniz Institute for Marine Sciences, Duesternbrooker Weg 20, 24105 Kiel, Germany. Phone: 49-431-600 4212. Fax: 11-49-431 600 4202. E-mail: jlaroche@ifm-geomar.de.

† Supplemental material for this article may be found at <http://aem.asm.org/>.

<sup>∇</sup> Published ahead of print on 1 February 2008.

TABLE 1. qPCR primers and TaqMan probes designed for this study

Type	Sequence (position) of <sup>a</sup> :			Reference sequence
	Primer		Probe	
	Reverse	Forward		
Group A	TCAGGACCACCGGACTCAAC (146–127)	TAGCTGCAGAAAGAGGAACT GTAGAAG (50–76)	TAATTCCTGGCTATAA CAAC (98–117)	AF059627.1
Filamentous	GCAAAATCCACCGCAAACAAC (275–256)	TGGCCGTGGTATTATTACTG CTATC (165–189)	AAGGAGCTTATACAGA TCTA (206–225)	AY896367.1
Group B	TCAGGACCACCAGATTCTAC ACACT (146–122)	TGCTGAAATGGGTTCTGT TGAA (54–75)	CGAAGACGTAATGCTC (87–102)	AY896454.1
Group C	GGTATCCTTCAAGTAGTACTT CGTCTAGCT (112–83)	TCTACCCGTTTGATGCTACAC ACTAA (1–26)	AAACTACCATTCTTCACT TAGCAG (32–55)	AY896461.1
Gamma A	AAAATGTAGATTTCTGAG CCTTATTC 321–294	TTATGATGTTCTAGGTGA TGTG (240–266)	TTGCAATGCCTATTTCG (275–292)	AY896371.1
Gamma P	CATCGCGAAACCACCAC ATAC (282–262)	TTGTGCAGGTCGTGGTGT AATC (159–180)	CCTATGACGAAGACCT AGAC (212–231)	AY896428.1
Cluster III	GCAGACCACGTACCCA GTAC (267–247)	ACCTCGATCAACATGCT CGAA (175–195)	CCTGGACTACGCGTTC (225–240)	AY896461.1

<sup>a</sup> All positions and sequences relate to the 324-base *nifH* segment length (5'→3').

without prescreening to remove large particles. One to two liters of seawater was filtered per sample during the two *Meteor* and *Poseidon* cruises. Two to seven liters of seawater was filtered during the *Sonne* cruise. After filtration, filters were frozen at  $-80^{\circ}\text{C}$  until extraction in the lab. Detailed information on some of the *Sonne* 152, *Poseidon* 284, and *Meteor* 55 stations can be found in reference 22. Nutrient samples from the *Meteor* 55 and 60 and the *Poseidon* 284 cruises were measured onboard using the methods described in reference 15.

All samples were extracted using the Qiagen DNeasy mini plant kit according to the manufacturer's protocol, except that the DNA was eluted two times with 50  $\mu\text{l}$  of prewarmed PCR-grade water. DNA concentrations were measured using the PicoGreen double-stranded DNA quantitation reagent (Molecular Probes) and a Fluoroscan Ascent microplate reader (Laborsystems) following the manufacturer's protocol. Amplicons of the *nifH* gene were produced using the previously described primers (45), amplified, and cloned (22).

**Primer selection.** Based on *nifH* sequence information from a subset of the samples (22), primers and TaqMan MGB probes (6-carboxyfluorescein reporter) were selected to target seven diazotroph phylotypes using Primer Express (version 2.0; Applied Biosystems) (Table 1). All primers and probes were checked against the NCBI database with a BLAST search to ensure that they did not contain any near perfect sequence matches, other than the selected phylotypes. Standards for the different phylotypes were obtained by cloning the environmental sequences for each phylotype into Top10 cells. Plasmid extraction and purification was done using the Qiagen plasmid purification kit according to the manufacturer's instructions. Plasmid DNA concentrations were measured with NanoDrop ND-1000 (PeqLab) and diluted to 4  $\mu\text{g } \mu\text{l}^{-1}$ , which corresponds to  $10^7$  target sequence copies in a 5- $\mu\text{l}$  volume. Serially diluted plasmid standards for filamentous, unicellular group A, unicellular group B, *Cyanotheca*-like (group C), gammaproteobacterium AO (gamma A), gammaproteobacterium PO (gamma P), and cluster III phylotypes were used to calculate copy numbers in the qPCR assays. The group B and gammaproteobacterial primers and TaqMan probes from our study were very different from those previously reported (10), while the filamentous and group A primers and probes from reference 10 detected a segment of the *nifH* gene similar to that detected in our study. Although independently designed, the reverse primer and probe for cluster III in our study were almost identical to those described in references 9 and 10. The group C primer and probe set designed for this study selected for a different part of the group C sequence than the set described in Foster et al. (13).

**qPCR assays and detection limits.** All qPCRs were run on an ABI Prism 7000 (Applied Biosystems) using the default cycling program, but increasing the number of cycles to 45. The program's cycling conditions were 2 min at  $50^{\circ}\text{C}$ , 10 min at  $95^{\circ}\text{C}$ , and 45 cycles of  $95^{\circ}\text{C}$  for 15 s, followed by 1 min at  $60^{\circ}\text{C}$ . The specificity of the qPCR primer and probe sets was confirmed by testing for cross-reactivity and sensitivity against each standard diluted to  $10^4$  and  $10^5$  *nifH* copies. DNA amplification signals were detected only for the homologous phylotype. It is important to note that the filamentous primer and probe set was designed for *Trichodesmium*, but due to the high similarity in the filamentous *nifH* sequences it amplified *Katagnymene* equally well. Additionally, the sensitivity of the primers and probes in a mixed-DNA sample was tested in combinations of serially diluted

standards mixed in ratios ranging from  $10^7:10^1$  to  $10^1:10^7$  copies of the specific and unspecific standard. There were no significant changes in the linear regressions, indicating that the presence of various amounts of closely related DNA sequences does not affect the quantification of a specific phylotype. However, the detection limit of the filamentous primer and probe set was 100 filamentous *nifH* copies when mixed with  $10^7$  group A *nifH* copies, a situation that was not observed in any samples.

qPCR mixtures contained  $1 \times$  TaqMan PCR buffer (Applied Biosystems), 100 nM TaqMan probe, 5 pmol/ $\mu\text{l}$  each of the forward and reverse primers, 400 ng/ $\mu\text{l}$  bovine serum albumin (BSA), 3  $\mu\text{l}$  PCR water, and 5  $\mu\text{l}$  of either standard or environmental sample (which corresponded to 1 to 6 ng environmental DNA, with an average of 2 ng). To test environmental samples for PCR inhibition, serial dilutions of several samples from each cruise were run. The results indicated different levels of inhibition in almost all samples tested. Also, additions of environmental DNA to standards resulted in an underestimation of the true copy number. Dilution of the samples partially reduced PCR inhibition but affected the detection limit. Inhibition of PCR is a common problem with environmental samples and has been reported before in other studies, which estimated the degree of the inhibition from qPCR efficiency without relieving the inhibition (13). Addition of BSA to the reaction consistently relieved the inhibition without affecting the standard curves or detection limit (data not shown). We therefore routinely added BSA to all qPCR mixtures. Environmental DNA samples were run in triplicate. The coefficient of variation for the cycle threshold ( $C_T$ ) value of all samples was 1.77% ( $n = 251$ ). Standards were serially diluted ( $10^7$  to  $10^1$  copies) and run in duplicate. The prepared serial dilutions were stored at  $4^{\circ}\text{C}$  and were stable for about 1 month. Standard curves from stored standard serial dilutions were highly reproducible and varied daily by an average  $C_T$  of 0.7. In contrast, freeze-thaw cycles of samples and standards resulted in 10-fold decrease in copy numbers (results not shown). To avoid this, extracted DNA was frozen in aliquots and thawed only once for qPCR determination.

No-template controls were run in duplicate for each primer and probe set and were undetectable after 45 cycles, thus setting the theoretical detection limit of our assay mixture to one *nifH* copy. However, the realized detection limit depends on the amount of seawater filtered per sample, elution volume after extraction, and the amount of sample loaded. In this study, the amount of seawater filtered determined the detection limits and these are 20, 50, and 75 copies liter $^{-1}$  of seawater for *Sonne*, *Poseidon*, *Meteor* 55, and *Meteor* 60 samples, respectively. Thus, in our assays, samples with a  $C_T$  value below 36, which corresponded to  $<100$  copies liter $^{-1}$ , were considered detectable but not quantifiable. To minimize potential differences between qPCRs run on different days, a sample was quantified with all primer and probe sets on 1 day and the same standard serial dilutions were used for all samples. The ABI 7000 system SDS software (version 1.2.3) with RQ study application was used to calculate linear regressions of  $C_T$  versus  $\log_{10}$  *nifH* standard copy numbers. PCR efficiencies were calculated using the formula  $E = 10^{-1/\text{slope}} - 1$  (1). Average PCR efficiencies were  $96.5\% \pm 2\%$  ( $n = 37$ ;  $R^2 = 0.999$ ) for filamentous,  $94.9\% \pm 1\%$  ( $n = 39$ ;  $R^2 = 0.999$ ) for group A,  $96.1\% \pm 2\%$  ( $n = 22$ ;  $R^2 = 0.997$ ) for group B,  $89.1\% \pm 6\%$  ( $n = 24$ ;  $R^2 = 0.998$ ) for group C,  $95.3\% \pm 2\%$  ( $n = 24$ ;  $R^2 = 0.998$ ) for

TABLE 2. Comparison of clone libraries and qPCR data given as percentages of each phylotype from the total number of either clones or phylotypes detected

Phylotype	% of clones recovered <sup>a</sup>	% of <i>nifH</i> copies detected from:	
		Samples with clone libraries <sup>b</sup>	All samples <sup>c</sup>
Filamentous	57.4	71.1	53.1
Group A	26.9	23.9	34.1
Group B	1.4	0.3	4.3
Group C	3.6	1.2	2.3
Gamma A	5.9	2.8	5.3
Gamma P	2.5	0.7	0.6
Cluster III	2.2	0.05	0.4

<sup>a</sup> A total of 357 clones was obtained from 23 cloned samples.

<sup>b</sup> A total of  $4.9 \times 10^6$  *nifH* copies liter<sup>-1</sup> was detected in samples with a corresponding clone library.

<sup>c</sup> A total of  $1.1 \times 10^7$  *nifH* copies liter<sup>-1</sup> was detected in all 142 samples.

gamma A,  $100\% \pm 2\%$  ( $n = 14$ ,  $R^2 = 0.997$ ) for gamma P, and  $100\% \pm 1\%$  ( $n = 22$ ;  $R^2 = 0.994$ ) for cluster III. Statistical analyses (Kruskal-Wallis and Mann-Whitney U tests) were performed with Statistica (version 6). *P* values of  $<0.05$  were considered significant. Maps of the distribution and abundance of *nifH* phylotypes in the North Atlantic were generated with Ocean Data View (37).

## RESULTS

**Sampling and DNA concentrations.** A total of 141 DNA samples were collected from four cruises to the northern Atlantic Ocean. Sixty-four samples were collected in surface waters, 41 from depths of 20 to 80 m, and 36 from depths below 80 m. Water temperatures from all samples ranged from 15 to 30°C, with the coldest (15 to 23°C) and highest (25 to 29°C) temperatures recorded during the *Meteor* 60 and *Meteor* 55 expeditions, respectively. All samples were collected in waters with a salinity of 34.6 to 37.2 ppt, with the exception of samples from four stations located in the Amazon River plume, where surface water salinities ranged between 31.2 and 33.4 ppt. NO<sub>3</sub> concentrations ranged from 0 to 25 μM; however, 65% of the samples were collected from waters with 0 to 1 μM NO<sub>3</sub>. PO<sub>4</sub> concentrations ranged from 0 to 1.5 μM, and 75% of the samples had concentrations of 0.25 μM PO<sub>4</sub> or less. DNA concentrations ranged from 16 ng liter<sup>-1</sup> to 640 ng liter<sup>-1</sup> (average, 132 ng liter<sup>-1</sup>). The lower DNA concentrations generally came from samples collected at depth. The *Sonne* and *Meteor* 55 samples collected with an overboard pump had on average a higher DNA concentration (237 ng liter<sup>-1</sup>) than samples collected with a CTD rosette (114 ng liter<sup>-1</sup>). No other trends were observed between DNA concentrations and location, depth, or time of year.

**Comparison of clone libraries versus qPCR.** Cyanobacterial phylotypes were the most abundantly detected diazotrophs (93.8% of the total *nifH* copies detected), with the majority being the filamentous phylotype (Table 2). The group A phylotype was the next most abundant, followed by gamma A, which was lower by 1 order of magnitude. The gamma P and cluster III phylotypes made up about 1% of all *nifH* sequences detected. These results reflect the relative abundance of phylotypes in clone libraries (22), except that rare groups detected at low abundance with qPCR were overestimated in pooled clone libraries. In direct comparisons of qPCR data and clone libraries from the same station, more diazotroph phylotypes

were detected with qPCR, thus demonstrating the higher sensitivity of this technique, especially for the detection of rare phylotypes. For 10 of the samples, which contained low diversity (two to three phylotypes present), the relative abundance of phylotypes from the cloned library accurately (5% difference) reflected abundances obtained with qPCR, except that groups with low copy numbers were sometimes absent from the clone libraries. However, results from qPCR and clone libraries diverged greatly for samples containing high (more than three phylotypes present) *nifH* diversity, with minor phylotypes completely absent from the clone library and large over- or underestimates of more dominant groups based on data from clone libraries. Results showed that qPCR provided a highly sensitive and quantitative estimate of phylotype abundance, in contrast with clone libraries, which can only show relative abundances at best (Table 2).

**Distributions of *nifH* phylotypes.** Diazotroph phylotypes were detected throughout the northern Atlantic Ocean (Fig. 1a). In general, very low to undetectable *nifH* copy numbers were observed along the equator and at latitudes higher than 30°N. The highest *nifH* copy numbers were measured in *Poseidon* samples between 18 to 30°N and 30 to 23°W; however, the lowest diversity was also observed at this location. High copy numbers and high diversity were detected in *Sonne* samples between 50 and 34°W and 2 and 15°N. The filamentous, group A, and gamma A phylotypes were the most commonly detected phylotypes and were distributed throughout the North Atlantic (Fig. 1b, e, and f). Both gammaproteobacterial and cluster III phylotypes were only detectable at low copy numbers (Fig. 1b to d). In contrast to the other phylotypes, the cluster III distribution reached as far as 40°N (Fig. 1d). This rare phylotype was detectable in *Sonne* and *Meteor* 60 samples, but only west of 33°W. Copy numbers ranged from the detection limit to 1,600 cluster III *nifH* copies liter<sup>-1</sup>, with the highest copy numbers measured at northern stations where the spring bloom was in progress (29). The gamma P phylotype occurred mainly in *Sonne* samples, and occasionally in *Poseidon* samples and the *Meteor* 55 samples, which were collected using a pump. In contrast, the gamma A *nifH* phylotype was detectable in most samples from all cruises, and ranged between 10<sup>3</sup> (*Sonne*) and 10<sup>4</sup> (*Meteor* 55) *nifH* copies liter<sup>-1</sup>.

Filamentous diazotroph *nifH* copy numbers were found north of the equator to about 15°N (Fig. 1e) and reached the highest abundances between 52°W and 35°W, though areas of high abundances were also present in the eastern part of the North Atlantic basin (up to 10<sup>6</sup> copies liter<sup>-1</sup>). Others have also observed higher abundances of *Trichodesmium* in the western Atlantic basin (12) than in the eastern basin. The filamentous phylotype was found at low copy numbers between 20°N and 30°N, and it was undetectable along the northern cruise track, except at the two southernmost stations (approximately 22°N).

Unicellular cyanobacterial diazotroph copy numbers were more variable than filamentous copy numbers. Group A unicellular cyanobacterial phylotypes were present throughout the study area and reached high concentrations (up to 10<sup>6</sup> group A *nifH* copies liter<sup>-1</sup>) (Fig. 1f). No group A *nifH* copies were detectable in the northwestern quadrant of the Atlantic Ocean (west of 30°W and north 17°N) during spring. Group A copy numbers were moderately high ( $9 \times 10^3$  to  $2 \times 10^4$  group A

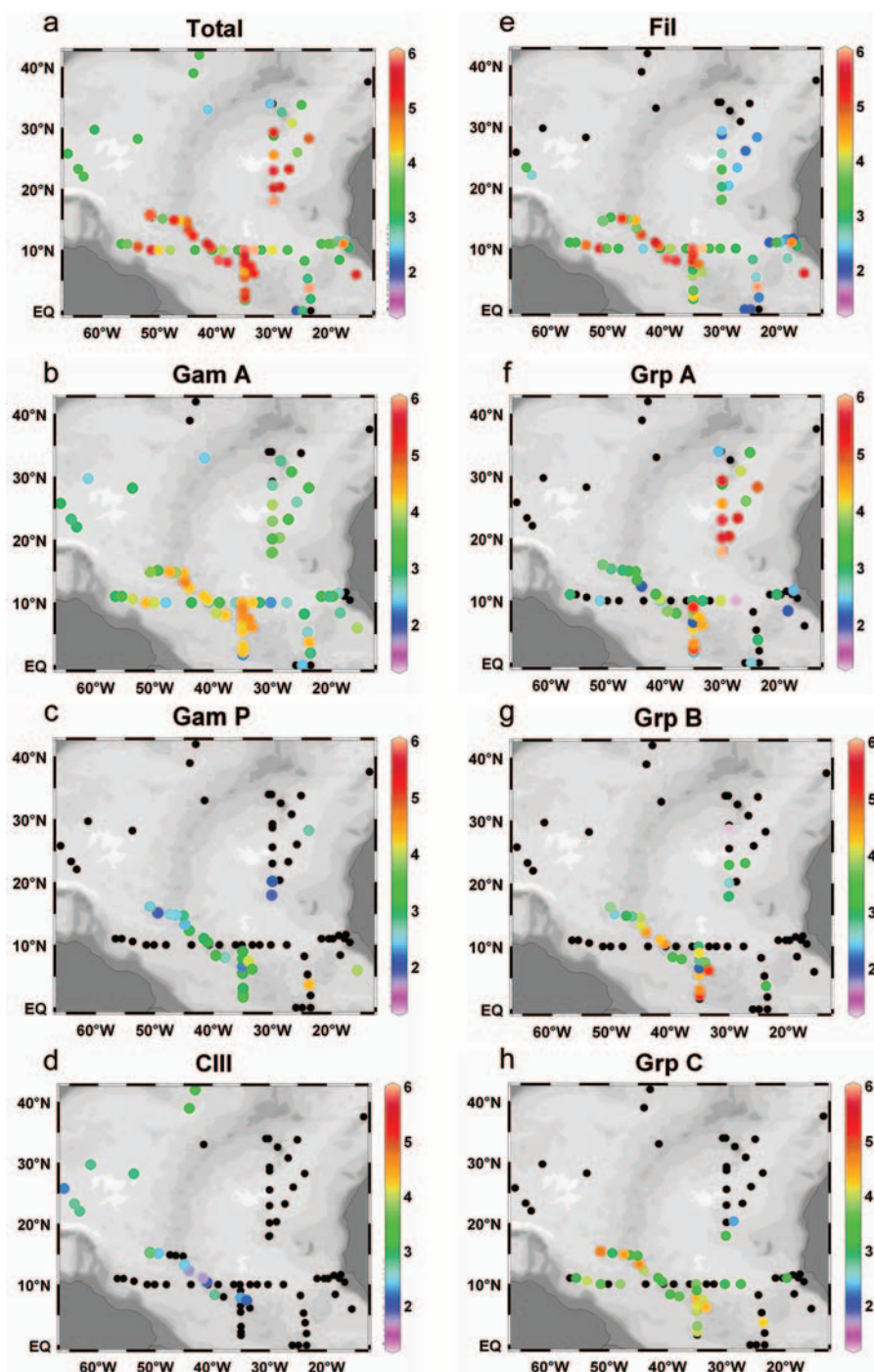


FIG. 1. Total *nifH* copies liter<sup>-1</sup> detected at each station (a) and *nifH* copies liter<sup>-1</sup> of each phylotype in panels b to h were plotted using Ocean Data View (37). Black dots indicate samples with concentrations below the detection limit. Note that the color scale is a log scale. Fil, filamentous; Gam, gamma; Grp, group; CIII, cluster III.

*nifH* copies liter<sup>-1</sup>) between the equator and 15°N but reached the highest abundances between 30°W to 23°W and 30°N to 17°N (*Poseidon* cruise track), where copy numbers ranged from  $4 \times 10^5$  to  $10^6$  copies liter<sup>-1</sup>. Group C *nifH* copy numbers were low to undetectable throughout the study area, except for some *Sonne* samples. Group B unicellular phylotypes were mainly found in *Sonne* samples, as well, but at higher concentrations:

$3 \times 10^4$  group B *nifH* copies liter<sup>-1</sup> as opposed  $1 \times 10^4$  group C *nifH* copies liter<sup>-1</sup> (Fig. 1g and h). No quantifiable group B or group C phylotypes were detected north of 20°N. The group B phylotype accounted for 6.9% of the total *nifH* copies detected in our samples, despite being detected at only 27 stations.

In an attempt to identify what factors influence the distri-

TABLE 3. Effect of sampling depth and NO<sub>3</sub> concentration on the abundance of *nifH* phylotypes<sup>a</sup>

Type <sup>b</sup>	% of <i>nifH</i> phylotype copies detected			
	Surface samples	Depth samples	<0.5 μM NO <sub>3</sub>	>0.5 μM NO <sub>3</sub>
Filamentous*†	99.2	0.8	99.5	0.5
Group A†	30.7	69.3	97.5	2.5
Group C*†	90.5	9.5	96.5	3.5
Gamma A*†	89.0	11.0	95.8	4.2
Gamma P	0.0	100.0	89.8	10.2
Cluster III	24.6	75.4	40.2	59.8
Total*†	94.1	5.9	97.9	2.1

<sup>a</sup> Data are given as the percentage of either *nifH* phylotype copies detected in surface and depth samples (columns 1 and 2) or *nifH* phylotypes recovered in waters with less than or greater than 0.5 μM NO<sub>3</sub>. Surface samples (up to 30 m deep) and corresponding depth samples (from 30 to 200 m) were available for 37 stations, and no group B phylotypes were detected in these samples (columns 1 and 2). NO<sub>3</sub> measurements were available for 112 samples.

<sup>b</sup> Phylotypes whose concentrations were significantly different ( $P < 0.05$ , Mann-Whitney U test) in samples collected at depth than in surface samples are identified by \*, while those significantly affected by NO<sub>3</sub> concentrations are identified by †.

bution of diazotrophs, we considered sampling depth, dissolved inorganic nutrient concentrations, mixed layer depth, water temperature, geographical distribution, and Fe fertilization via mineral dust deposition. Comparison of paired surface (up to 30 m deep) and deep (30 to 200 m) samples from 37 stations indicated that overall total diazotroph abundance decreased with depth (Mann-Whitney U test;  $P = 0.004$ ). More specifically, the filamentous, gamma A, and group C phylotype concentrations were significantly higher in the surface samples (Mann-Whitney U test;  $P < 0.001$ ). There were a few stations where the group A phylotype was detected both at the surface and at depth; however, the majority of group A phylotypes were detected between 10 and 30 m. Cluster III and gamma P concentrations appeared to increase with depth, but this result was not statistically significant (Table 3).

Significant relationships were also observed between *nifH* distribution and residual NO<sub>3</sub> (Table 3) and PO<sub>4</sub> concentrations (results not shown), with most phylotypes being almost

completely restricted to NO<sub>3</sub> concentrations less than 0.5 μM. One clear exception was the cluster III phylotype, which showed no significant preference for low NO<sub>3</sub> waters (Table 3). Mixed-layer depth showed no direct relationship with specific *nifH* phylotypes (results not shown).

The influence of temperature on the distribution of *nifH* phylotypes was investigated by calculating the mean water temperature for each phylotype in samples containing greater than 100 *nifH* copies liter<sup>-1</sup>. The mean temperature for each phylotype ranged from 28°C for group C to 18°C for cluster III (Fig. 2a). We observed that most phylotypes were associated with narrow temperature ranges except for gamma P, the least abundant phylotype, which appeared to be poorly constrained by temperature. The group C phylotype was detected in very warm waters, while gamma A, gamma P, and group B were detected mainly in waters of about 24°C. Temperature means for group C, filamentous, gamma A, and cluster III were significantly different from the mean water temperature of all samples. Interestingly, cluster III was the only phylotype whose mean detection temperature was below the mean of all samples. The clearest associations between temperature and *nifH* phylotypes were for the filamentous and group A phylotypes, which were detected in significant quantities at average temperatures of 26°C and 20.9°C, respectively (Fig. 2a). Although the filamentous and group A phylotypes were detected throughout the temperature range, the highest copy numbers were detected in samples with water temperatures from 28 to 30°C and 19 to 24°C, respectively (Fig. 2b). This suggests that these two dominant groups may have different temperature optima.

**Distribution by geographical areas.** The large geographical coverage of our data prompted us to analyze the distributions and abundances of the *nifH* phylotypes in six regions (Fig. 3a), defined as a function of the basic water characteristics, temperature and salinity, of the surface water sample (see Fig. S1 in the supplemental material). Average *nifH* gene copy numbers for the stations within regions A, B, and C, corresponding to areas north of 35°N, the equator, and the Sargasso Sea respectively, contained very low abundances of potential diazotrophs (Fig. 3b). In contrast, the highest average surface and

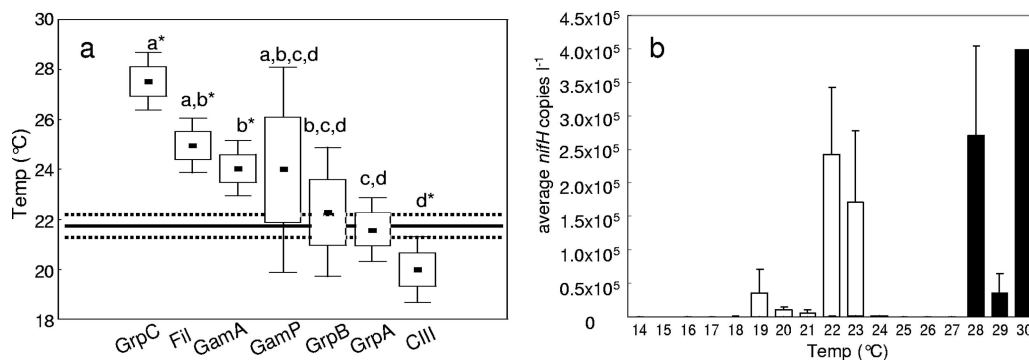


FIG. 2. Box-whisker plots (black dots, mean; boxes, standard error; bars, 95% confidence interval) show the temperatures where >100 *nifH* copies liter<sup>-1</sup> were detected for all phylotypes in panel a. The mean temperature of all samples (22°C) and the associated standard error are indicated by a black line and dashed line, respectively. Phylotype temperature means which are significantly different from 22°C ( $P < 0.05$ , Kruskal-Wallis test) are identified by asterisks. Letters signify groups of phylotypes whose temperature means are not significantly different from another group (Mann-Whitney U test). Average filamentous and group A *nifH* copies liter<sup>-1</sup> detected at sample temperatures rounded to the nearest whole degree are displayed in panel b. Error bars indicate the standard error.

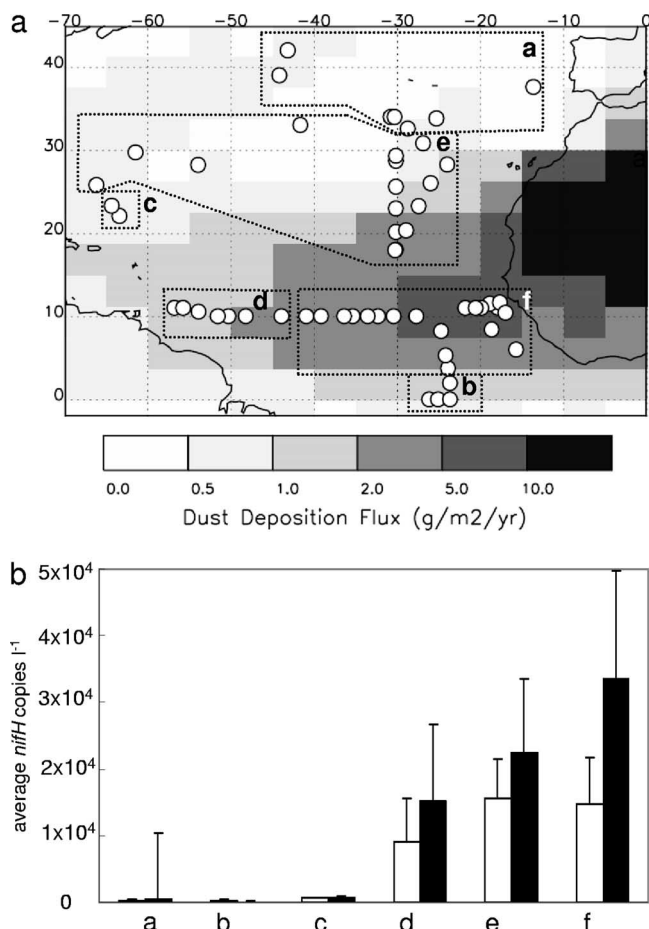


FIG. 3. Separation of stations according to geographical location (a) and physical characteristics (see the supplemental material). Station locations are overlaid on a map of predicted annual dust deposition. The average number of *nifH* copies liter<sup>-1</sup> and standard error from all samples (clear bars) and only surface samples (black bars) in each region are plotted in panel b. Region letters correspond to the panels in Fig. 4. Some 152 samples were not plotted because no temperature and salinity data were available.

total *nifH* gene copy numbers were detected in regions E and F (Fig. 1a and 3b).

For each geographical area, average *nifH* concentrations of individual phylotypes were plotted versus temperature (Fig. 4). Region A (northerly stations) was characterized by low surface water temperatures (<19°C) and relatively high salinity (>36.2 ppt). This area of very low *nifH* gene copy numbers (Fig. 3 and 4a) contained only the cluster III, group A, and gamma A phylotypes. Of the eight samples measured in region B (equator), only one contained abundances well above the detection limit (Fig. 4b). Here, diversity was low and only the filamentous and a few gamma A phylotypes were detected. Stations in the Sargasso Sea were sampled in the spring time (region C, Fig. 4c), exhibited deep mixed layers, and contained low *nifH* concentrations. The three phylotypes found there consisted of the rare cluster III phylotype as well as the gamma A and filamentous phylotypes. These phylotypes were homogeneously distributed throughout the stations, even at depths up to 160 m. Region D contained samples that were influenced by the

Amazon River, where surface water temperatures were greater than 28°C and diazotroph concentrations, especially the filamentous phylotype, were higher in the surface samples (Fig. 4d).

Total *nifH* concentrations were relatively similar in regions E and F (Fig. 3b), but different groups were dominant (Fig. 4e and f'). Region E samples were characterized by surface water temperatures of 20 to 23°C and salinity of 36.8 to 37 ppt. This area was dominated by the group A phylotype. The cluster III phylotype was also detected, but only in the samples from the western half of this region. In contrast, the filamentous phylotype dominated region F, where surface water temperatures were greater than 27°C and the salinity was 34.7 to 35.6 ppt.

The amount of dust deposition may play a role in determining the abundance and distribution of diazotrophs in a certain region. In Fig. 3a, the stations are plotted in relation to the annual dust deposition. Samples were then grouped according to estimated annual dust deposition (Fig. 5). The highest diazotroph concentrations were detected where the dust deposition was between 2 and 5 g m<sup>-2</sup> year<sup>-1</sup> (Fig. 5). The geographical regions with the lowest number of *nifH* copies detected (i.e., all of region A and most of region B samples) were located in the modeled dust deposition area with <1 g m<sup>-2</sup> year<sup>-1</sup>. Only the cluster III phylotype was detected more often in regions with low dust deposition (Fig. 1d and 5).

## DISCUSSION

**Assessing relative diversity and phylotype abundances from qPCR data.** Although extensive sequencing of clone libraries generated from endpoint PCR products has the potential to uncover rare and new phylotypes, amplification biases can occur from preferential primer binding, the use of different types of *Taq* polymerases (32), nonselection by a primer set (30), and multiple target gene copies. For this reason, it is well recognized that endpoint PCR techniques are not suitable for quantitative analysis of genetically diverse phylotypes from natural microbial communities. Prior knowledge of the *nifH* gene diversity from the study area (22) allowed us to target and quantitatively estimate the abundance of the dominant phylotypes, avoiding amplification biases by using specific primer and probe sets. We found that an approach combining both sequence analyses from clone libraries and TaqMan-based qPCR assays was needed for accurately assessing both diversity and abundances of diazotrophs in a given environment.

The presence of multiple gene copies in the genome of an organism as well as multiple genome copies per cell can affect the extrapolation of qPCR results to estimates of cell abundance. It is known that some diazotrophs, such as *Clostridium pasteurianum*, have multiple copies of the *nifH* gene (35). Others, such as *Trichodesmium erythraeum* and *Crocospaera watsonii*, have only one copy of the *nifH* gene per genome. As there is no available genome information for the uncultured phylotypes and little information on the variability of genome copies per cell for all *nifH* phylotypes, the concentrations of *nifH* genes presented in this study should be considered an upper limit of the cell density. Given the limited dissolved P and N supply in the euphotic zone of the oligotrophic North Atlantic (27, 44), the presence of multiple genome copies per cell is unlikely. In contrast, this may be a consideration for

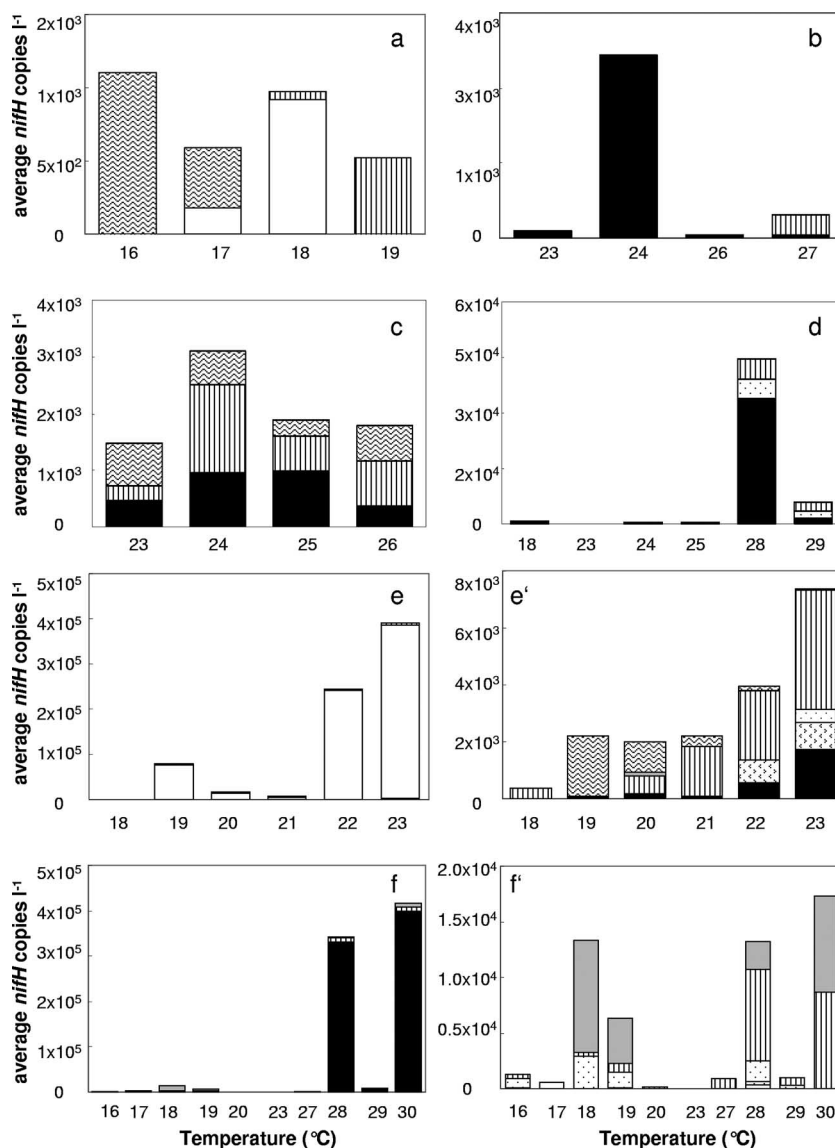


FIG. 4. Average concentrations of *nifH* copies liter<sup>-1</sup> by sample temperature (rounded to the nearest whole degree) in each geographic location are shown, with panel letters corresponding to the regions in Fig. 3. ■, filamentous; □, group A; ▨, group B; ▩, group C; ▪, gamma A; ▫, gamma P; and ⊙, cluster III. The numbers of samples for regions a, b, c, d, e, and f are 21, 8, 6, 40, 105, and 96, respectively. Panels e' and f' show the average numbers of *nifH* copies liter<sup>-1</sup> from panels e and f without the dominant group A and filamentous phylotypes, respectively.

diazotrophs located below the euphotic zone, where nutrient levels are high (26).

**Diazotrophic communities of the Atlantic Ocean.** Our results on *nifH* phylotype distribution emphasize the importance of *Trichodesmium* in the tropical Atlantic Ocean, complementing other studies (6), as filamentous *nifH* sequences made up 51% of all detected sequences. Filamentous concentrations were similar to *Trichodesmium* cell counts (7). Although the distribution of *Trichodesmium* exhibits a latitudinal trend with increasing abundances in southerly latitudes, seasonality may also play an important role in explaining the distribution patterns of this phylotype in our study. Nitrogen fixation rates have been reported to be highest during the late summer and autumn and lowest in the winter in the area above 10°N and

west of 40°W (6). The two cruises with the highest filamentous copy numbers (*Sonne* and *Meteor* 55) were during the fall. The *Meteor* 60 cruise was during the spring, the season corresponding to the lowest *Trichodesmium* abundances in this latitudinal range (31).

Although filamentous phylotypes were dominant in our study, the group A unicellular phylotype was responsible for over a third of our total *nifH* copies, suggesting that this group may periodically contribute significantly to N<sub>2</sub> fixation in the northern Atlantic. The gamma A phylotype, although detected at low concentrations, was found in almost all samples and may also play an important role globally due its widespread distribution. It has already been demonstrated that gammaproteobacteria are cosmopolitan (8), and an *nifH* gammapro-

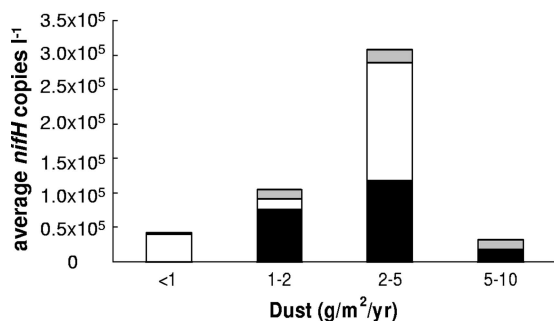


FIG. 5. Average concentrations of *nifH* copies liter<sup>-1</sup> for filamentous (■), group A (□), and all other phylotypes combined (gray square) as a function of estimated annual dust deposition are shown. Average temperatures of each region were 22.3°C (5 to 10 g m<sup>-2</sup> year<sup>-1</sup>), 24.5°C (2 to 5 g m<sup>-2</sup> year<sup>-1</sup>), 26.8°C (1 to 2 g m<sup>-2</sup> year<sup>-1</sup>), and 19.3°C (<1 g m<sup>-2</sup> year<sup>-1</sup>). The dust deposition map was provided by I. Tegen, using the data from reference 42.

teobacterial sequence 99% similar to the gamma A target sequence of this study was present at all stations in an Arabian Sea study (4). Taken together, these results suggest that the widespread distribution of *nifH* phylotypes belonging to the gammaproteobacterial group warrants further study of its role in the global nitrogen cycle.

The presence of cluster III *nifH* phylotypes in oxygenated low light waters with detectable to high nitrate is puzzling. In our study, the highest concentrations of cluster III phylotypes were detected during the spring bloom at stations characterized by a deep mixed layer and high nitrate concentrations (29), suggesting that high nitrate conditions do not select against all diazotrophs (20). Even *Trichodesmium*, which in our study was abundant only in oligotrophic waters, could retain some ability to fix nitrogen when grown in cultures with high nitrate concentrations (18). Diverse cluster III *nifH* transcripts, distantly related (<60%) to the ones described here, have also been reported in well-oxygenated surface waters of the Mediterranean Sea (24). It was suggested that cluster III diazotrophs from oxygenated waters may be either facultative anaerobes or associated with zooplankton (24). Photosynthetic, diazotrophic, purple sulfur bacteria have been reported in association with copepods and have been found to fix nitrogen (34). Although prefiltered (10 μm) samples preclude zooplankton as the host of cluster III phylotypes in some studies (9), a zooplankton-cluster III association cannot be ruled out in the present study. Whether cluster III contributes significantly to global nitrogen fixation remains an open question requiring further work.

To date there have been few other studies which have looked at the distribution of oceanic diazotrophs quantitatively. Published concentrations of diazotroph phylotypes (9, 10) measured by real-time qPCR were comparable to those obtained in this study. Church et al. (9) reported the group A phylotype as being the most numerous (2 × 10<sup>5</sup> copies liter<sup>-1</sup>) in upper waters and the cluster III phylotype abundant in dim waters (100 to 1,000 copies liter<sup>-1</sup>). The situation was different in the Atlantic Ocean, with some stations dominated by the filamentous phylotype and cluster III often undetectable even at depth. Concentrations reported by Foster et al. (13) of the filamentous, group A, group B, and group C phylotypes were

comparable to those detected in region D. We did not observe any *nifH* sequences related to the diatom-diazotroph symbiont *Richelia* in our clone libraries and therefore did not quantify these groups, although our samples were collected from waters with higher salinities and lower Si concentrations (0 to 1 μM) than those where Foster et al. (13) observed the diatom-diazotroph association. The Sargasso Sea has been considered an area where nitrogen fixation can be important (31); however, we detected low *nifH* copy numbers in this area (region C), a finding shared by others (17).

In our study, filamentous and group A were the dominant phylotypes whose distributions were well separated as a function of temperature (Fig. 2). The filamentous and group A phylotypes were dominant at stations with water temperatures ranging between 28 and 30°C and 22 and 23°C, respectively. Similarly, group A dominated at the ALOHA time series site when the water temperature ranged between 23 and 24°C (9, 22). The direct effects of temperature on the physiology of an organism can be confounded by the role temperature plays in water column stratification, light regimens, and nutrient availability. In the case of *Trichodesmium*, the association with high water temperature reflects a direct effect on nitrogen fixation and growth rates, with the optima for both physiological processes occurring between 24 and 30°C (5, 40). The physiological reasons for this high temperature preference are not completely understood (41). A combination of factors such as lower dissolved O<sub>2</sub> concentration and a higher respiration rate at high temperatures may favor *Trichodesmium* growth by facilitating O<sub>2</sub> scavenging and thereby protecting nitrogenase against irreversible O<sub>2</sub> damage. A change from 30°C to 20°C waters would result in a 20% increase in dissolved O<sub>2</sub> concentration and in a twofold reduction in respiration rates. Except for a few sparse field observations, there are currently no data for the other *nifH* phylotypes primarily because there are no culture isolates. It is therefore not possible at this stage to establish the effects of temperature on organism physiology for the other diazotrophic groups, although there is a need to carry out laboratory experiments with a group B isolate, *C. watsonii*.

The detection of *nifH* in a DNA sample gives an estimate of the potential for diazotrophy within the microbial community. Whether any of the detected diazotrophs were actively fixing dinitrogen cannot be determined from our results, as only information on *nifH* DNA copy numbers is presented here. However, dinitrogen fixation rates ranging from 3.7 to 255 μmol m<sup>-2</sup> day<sup>-1</sup> were measured during the same cruises (27, 43), indicating that some of the *nifH* phylotypes were actively fixing N<sub>2</sub>.

***nifH* distribution relative to dust deposition.** Iron supply has been shown to limit diazotrophic growth (33) and, in combination with phosphate, nitrogen fixation (27). This limitation is probably because diazotrophs can have an iron requirement up to 10 times greater than that of other photoautotrophs (21, 40) which is needed for the synthesis of the nitrogenase enzyme. Iron is supplied to the Atlantic Ocean mainly through deposition of aeolian dust, originating from the Sahara (19). The concentration of *nifH* phylotypes was higher in regions which receive an estimated annual dust deposition of 2 to 5 g m<sup>-2</sup> year<sup>-1</sup> than in the area with 5 to 10 g m<sup>-2</sup> year<sup>-1</sup>. Trichomes were indeed visible in water samples and on filters in the area with 2 to 5 g m<sup>-2</sup> year<sup>-1</sup>. Although the western coast of Africa

receives the largest amount of dust, seasonal upwelling brings colder temperatures and higher macronutrient concentrations, which most likely favor groups other than diazotrophs, thus potentially explaining why *nifH* abundance was considerably lower in the area with dust deposition of 5 to 10 g m<sup>-2</sup> year<sup>-1</sup>. Dust particle size may also play a role in determining the bioavailability of Fe, with heavier particles deposited more quickly and sinking faster than finer particles (2). Similar to our findings, Voss et al. (43) found that nitrogen fixation rates were correlated with dissolved iron concentrations during the *Meteor 55* cruise. In contrast, a study focused on nitrogen fixation by *Trichodesmium* in the central North Atlantic found no correlation of N<sub>2</sub> fixation rates with dissolved iron (36). The authors concluded that *Trichodesmium* was not iron limited in their study because of high dissolved iron concentrations observed in April, a month of high dust deposition. The cruise track from their study was mainly located within the area with a modeled annual dust deposition of 2 to 5 g/m<sup>2</sup>/year, covering a fraction of the geographical area presented in our study. Whether temperature, geographical location, residual NO<sub>3</sub>, or amount of dust deposition plays a larger role in determining the composition of diazotrophs requires further study.

**Conclusions.** Our study presents a snapshot of *nifH* phylo-type distribution and abundance covering a large geographical area of the North Atlantic and expands the known distribution range of diazotrophs. The dominant phylogenetic filamentous and group A had different temperature optima, indicating that these two groups may occupy different niches. Although most *nifH* phylogenetic types were associated with warm waters with very low NO<sub>3</sub> concentration, the presence of the cluster III phylogenetic types at relatively high latitudes and high NO<sub>3</sub> concentrations was unexpected. Data on nitrogenase activity or *nifH* expression will be needed to confirm that these *nifH* phylogenetic types actively fix dinitrogen in all of the locations where they were detected. There is currently no information on the seasonal distribution and diurnal activity of most *nifH* phylogenetic types, with the notable exception of *Trichodesmium* (10). Our study suggests that atmospheric mineral dust deposition and temperature are important factors determining the distribution and abundance of the various *nifH* phylogenetic types. However, confirmation of our observations will require a coupled seasonal analysis of the *nifH* phylogenetic distribution and mineral dust deposition in the North Atlantic.

#### ACKNOWLEDGMENTS

We thank the captains and crews of the F/S *Meteor* and *Poseidon* and chief scientists D. Wallace (*Meteor 55* and 60 expeditions) and P. Kähler (*Poseidon 284*). We thank I. Tegen for providing the dust deposition map and F. Malien for nutrient analyses. We thank two anonymous reviewers for constructive comments.

This work was supported by DFG grants RO 2138/4–1 and RO 2138/5–1 to J.L.

#### REFERENCES

- Atallah, Z. K., J. Bae, S. H. Jansky, D. I. Rouse, and W. R. Stevenson. 2007. Multiplex real-time quantitative PCR to detect and quantify *Verticillium dahliae* colonization in potato lines that differ in response to verticillium wilt. *Am. Phytopathol. Soc.* **97**:865–872.
- Baker, A. R., and T. D. Jickells. 2006. Mineral particle size as a control on aerosol iron solubility. *Geophys. Res. Lett.* **33**.
- Berman-Frank, I., P. Lundgren, and P. Falkowski. 2003. Nitrogen fixation and photosynthetic oxygen evolution in cyanobacteria. *Res. Microbiol.* **154**:157–164.
- Bird, C., J. Martinez Martinez, A. G. O'Donnell, and M. Wyman. 2005. Spatial distribution and transcriptional activity of an uncultured clade of planktonic diazotrophic  $\gamma$ -proteobacteria in the Arabian Sea. *Appl. Environ. Microbiol.* **71**:2079–2085.
- Breitbarth, E., A. Oschlies, and J. La Roche. 2006. Physiological constraints on the global distribution of *Trichodesmium*—effect of temperature on diazotrophy. *Biogeosciences*. [www.biogeosciences.net/3/1/2006/](http://www.biogeosciences.net/3/1/2006/).
- Capone, D., J. Burns, J. P. Montoya, A. Subramaniam, C. Mahaffey, T. Gunderson, A. F. Michaels, and E. J. Carpenter. 2005. Nitrogen fixation by *Trichodesmium* spp.: an important source of new nitrogen to the tropical and subtropical North Atlantic Ocean. *Global Biogeochem. Cycles*. doi:10.1029/2004GB002331.
- Carpenter, E. J., A. Subramaniam, and D. Capone. 2004. Biomass and primary productivity of the cyanobacterium *Trichodesmium* spp. in the tropical N Atlantic Ocean. *Deep-Sea Res.* **51**:173–203.
- Cho, J.-C., and S. J. Giovannoni. 2004. Cultivation and growth characteristics of a diverse group of oligotrophic marine *Gammaproteobacteria*. *Appl. Environ. Microbiol.* **70**:432–440.
- Church, M. J., B. D. Jenkins, D. M. Karl, and J. P. Zehr. 2005. Vertical distributions of nitrogen-fixing phylogenetic types at Stn ALOHA in the oligotrophic North Pacific Ocean. *Aquat. Microb. Ecol.* **38**:3–14.
- Church, M. J., C. M. Short, B. D. Jenkins, D. M. Karl, and J. P. Zehr. 2005. Temporal patterns of nitrogenase (*nifH*) gene expression in the oligotrophic North Pacific Ocean. *Appl. Environ. Microbiol.* **71**:5362–5370.
- Codispoti, L. A., J. A. Brandes, J. P. Christensen, A. H. Devol, S. W. A. Naqvi, H. W. Paerl, and T. Yoshinari. 2001. The oceanic fixed nitrogen and nitrous oxide budgets: moving targets as we enter the anthropocene? *Sci. Mar.* **62**:85–105.
- Davis, C. S., and D. J. McGillicuddy, Jr. 2006. Transatlantic abundance of the N<sub>2</sub>-fixing colonial cyanobacterium *Trichodesmium*. *Science* **312**:1517–1520.
- Foster, R. A., A. Subramaniam, C. Mahaffey, E. J. Carpenter, D. Capone, and J. P. Zehr. 2007. Influence of the Amazon River plume on distributions of free-living and symbiotic cyanobacteria in the western tropical north Atlantic Ocean. *Limnol. Oceanogr.* **52**:517–532.
- Fulweiler, R. W., S. W. Nixon, B. A. Buckley, and S. L. Granger. 2007. Reversal of the net dinitrogen gas flux in coastal marine sediments. *Nature* **448**:180–182.
- Grasshoff, K., M. Ehrhardt, and K. Kremling. 1983. *Methods of seawater analysis*. Springer-Verlag, New York, NY.
- Gruber, N., and J. L. Sarmiento. 1997. Global patterns of marine nitrogen fixation and denitrification. *Global Biogeochem. Cycles* **11**:235–266.
- Hewson, I., P. H. Moisaner, K. M. Achilles, C. A. Carlson, B. D. Jenkins, E. Mondragon, A. E. Morrison, and J. P. Zehr. 2007. Characteristics of diazotrophs in surface to abyssopelagic waters of the Sargasso Sea. *Aquat. Microb. Ecol.* **46**:15–30.
- Holl, C. M., and J. P. Montoya. 2005. Interactions between nitrate uptake and nitrogen fixation in continuous cultures of the marine diazotroph *Trichodesmium* (Cyanobacteria). *J. Phycol.* **41**:1178–1183.
- Jickells, T. D., Z. S. An, K. K. Andersen, A. Baker, G. Bergametti, N. Brooks, J. J. Cao, P. W. Boyd, R. A. Hunter, K. A. Kawahata, N. Kubilay, J. La Roche, P. S. Liss, N. Mahowald, J. M. Prospero, A. J. Ridgwell, I. Tegen, and O. Torres. 2005. Global iron connections between desert dust, ocean biogeochemistry, and climate. *Science* **308**:67–71.
- Karl, D., A. Michaels, B. Bergman, D. Capone, E. Carpenter, R. Letelier, F. Lipschultz, H. Paerl, D. Sigman, and L. Stal. 2002. Dinitrogen fixation in the world's oceans. *Biogeochemistry* **57**:47–98.
- Kustka, A., E. J. Carpenter, and S. A. Sanudo-Wilhelmy. 2002. Iron and marine nitrogen fixation: progress and future directions. *Res. Microbiol.* **153**:255–262.
- Langlois, R. J., J. La Roche, and P. A. Raab. 2005. Diazotrophic diversity and distribution in the tropical and subtropical Atlantic Ocean. *Appl. Environ. Microbiol.* **71**:7910–7919.
- Mahaffey, C., R. G. Williams, G. A. Wolff, N. Mahowald, W. Anderson, and M. Woodward. 2003. Biogeochemical signatures of nitrogen fixation in the eastern North Atlantic. *Geophys. Res. Lett.* **30**:1300.
- Man-Aharonovich, D., N. Kress, E. B. Zeev, I. Berman-Frank, and O. Beja. 2007. Molecular ecology of *nifH* genes and transcripts in the eastern Mediterranean Sea. *Environ. Microbiol.* **9**:2354–2363.
- Mazard, S. L., N. J. Fuller, K. M. Orcutt, O. Bridle, and D. J. Scanlan. 2004. PCR analysis of the distribution of unicellular cyanobacterial diazotrophs in the Arabian Sea. *Appl. Environ. Microbiol.* **70**:7355–7364.
- Mehta, M. P., D. A. Butterfield, and J. A. Baross. 2003. Phylogenetic diversity of nitrogenase (*nifH*) genes in deep-sea and hydrothermal vent environments of the Juan de Fuca ridge. *Appl. Environ. Microbiol.* **69**:960–970.
- Mills, M. M., C. Ridame, M. Davey, J. La Roche, and R. J. Geider. 2004. Iron and phosphorus co-limit nitrogen fixation in the eastern tropical North Atlantic. *Nature* **429**:292–294.
- Montoya, J. P., C. M. Holl, J. P. Zehr, A. Hansen, T. A. Villareal, and D. Capone. 2004. High rates of N<sub>2</sub> fixation by unicellular diazotrophs in the oligotrophic Pacific Ocean. *Nature* **430**:1027–1031.
- Moore, C. M., M. Mills, A. Milne, R. J. Langlois, E. P. Achterberg, K.

- Lochte, R. Geider, and J. La Roche. 2006. Iron limits primary productivity during spring bloom development in the central North Atlantic. *Global Change Biol.* **12**:626–634.
30. Nuebel, U., F. Garcia-Pichel, M. Kühl, and G. Muyzer. 1999. Quantifying microbial diversity: morphotypes, 16S rRNA genes, and carotenoids of oxygenic phototrophs in microbial mats. *Appl. Environ. Microbiol.* **65**:422–430.
31. Orcutt, K. M., F. Lipschulz, K. Gundersen, R. Arimoto, A. F. Michaels, A. H. Knap, and J. R. Gallon. 2001. A seasonal study of the significance of N<sub>2</sub> fixation by *Trichodesmium* spp. at the Bermuda Atlantic Time-series Study (BATS) site. *Deep-Sea Res. Part II* **48**:1583–1608.
32. Osborn, A. M., E. R. B. Moore, and K. N. Timmis. 2000. An evaluation of terminal-restriction fragment length polymorphism (T-RFLP) analysis for the study of microbial community structure and dynamics. *Environ. Microbiol.* **2**:39–50.
33. Paerl, H. W., L. E. Prufert-Bebout, and C. Guo. 1994. Iron-simulated N<sub>2</sub> fixation and growth in natural and cultured populations of the planktonic marine cyanobacterium *Trichodesmium* spp. *Appl. Environ. Microbiol.* **60**:1044–1047.
34. Proctor, L. 1997. Nitrogen-fixing, photosynthetic, anaerobic bacteria associated with pelagic copepods. *Aquat. Microb. Ecol.* **12**:105–113.
35. Rosado, A., G. F. Duarte, L. Seldin, and J. D. van Elsas. 1998. Genetic diversity of *nifH* gene sequences in *Paenibacillus azotofixans* strains and soil samples analyzed by denaturing gradient gel electrophoresis of PCR-amplified gene fragments. *Appl. Environ. Microbiol.* **64**:2770–2779.
36. Sañudo-Wilhelmy, S. A., A. B. Kustka, C. J. Gobler, D. A. Hutchins, M. Yang, K. Lwiza, J. Burns, D. G. Capone, J. A. Raven, and E. J. Carpenter. 2001. Phosphorus limitation of nitrogen fixation by *Trichodesmium* in the central Atlantic Ocean. *Nature* **411**:66–69.
37. Schlitzer, R. 2004. Ocean Data View, 2.0 ed. AWI, Bremerhaven, Germany.
38. Short, S. M., and J. P. Zehr. 2005. Quantitative analysis of *nifH* genes and transcripts from aquatic environments. *Methods Enzymol.* **397**:380–394.
39. Short, S. M., B. D. Jenkins, and J. P. Zehr. 2004. Spatial and temporal distribution of two diazotrophic bacteria in the Chesapeake Bay. *Appl. Environ. Microbiol.* **70**:2186–2192.
40. Staal, M., S. te Lintel Hekkert, P. Herman, and L. J. Stal. 2002. Comparison of models describing light dependence of N<sub>2</sub> fixation in heterocystous cyanobacteria. *Appl. Environ. Microbiol.* **68**:4679–4683.
41. Staal, M., F. J. R. Meysman, and L. J. Stal. 2003. Temperature excludes N<sub>2</sub>-fixing heterocystous cyanobacteria in the tropical oceans. *Nature* **425**:504–507.
42. Tegen, I., M. Werner, S. P. Harrison, and K. Kohfeld. 2004. Relative importance of climate and land use in determining present and future global soil dust emission. *Geophys. Res. Lett.* doi:10.1029/2003GL019216.
43. Voss, M., P. Croot, K. Lochte, M. Mills, and I. Peeken. 2004. Patterns of nitrogen fixation along 10°N in the tropical Atlantic. *Geophys. Res. Lett.* doi:10.1029/2004GL020127.
44. Wu, J., W. Sunda, E. A. Boyle, and D. M. Karl. 2000. Phosphate depletion in the western North Atlantic Ocean. *Science* **289**:759–762.
45. Zani, S., M. T. Mellon, J. L. Collier, and J. P. Zehr. 2000. Expression of *nifH* genes in natural microbial assemblages in Lake George, New York, detected by reverse transcriptase PCR. *Appl. Environ. Microbiol.* **66**:3119–3124.
46. Zehr, J. P., B. D. Jenkins, S. M. Short, and G. F. Steward. 2003. Nitrogenase gene diversity and microbial community structure: a cross-system comparison. *Environ. Microbiol.* **5**:539–554.
47. Zehr, J. P., M. T. Mellon, and S. Zani. 1998. New nitrogen-fixing microorganisms detected in oligotrophic oceans by amplification of nitrogenase (*nifH*) genes. *Appl. Environ. Microbiol.* **64**:3444–3450.
48. Zehr, J. P., J. P. Montoya, B. D. Jenkins, I. Hewson, E. Mondragon, C. M. Short, M. J. Church, A. Hansen, and D. M. Karl. 2007. Experiments linking nitrogenase gene expression to nitrogen fixation in the North Pacific subtropical gyre. *Limnol. Oceanogr.* **52**:169–183.
49. Zehr, J. P., and B. B. Ward. 2002. Nitrogen cycling in the ocean: new perspectives on processes and paradigms. *Appl. Environ. Microbiol.* **68**:1015–1024.